Available online at www.sciencedirect.com

SCIENCE DIRECT®

Palaeogeography, Palaeoclimatology, Palaeoecology 215 (2004) 17–36

PALAEO

www.elsevier.com/locate/palaeo

Comparison of the hydrological and hydrochemical evolution of Lake Naivasha (Kenya) during three highstands between 175 and 60 kyr BP

A.G.N. Bergner*, M.H. Trauth

Institut für Geowissenschaften, Universität Potsdam, POB 601553, Potsdam, Germany

Received 6 August 2003; received in revised form 1 July 2004; accepted 21 July 2004

Abstract

Three diatomite beds exposed in the Ol Njorowa Gorge south of Lake Naivasha, Central Kenya Rift, document three major lake-level highstands between 175 and 60 kyr BP. Diatom transfer-function estimates of hydrological and hydrochemical parameters suggest that a deep and large freshwater lake existed during the highstands at ~135 and ~80 kyr BP. In contrast, a shallower but more expanded freshwater lake existed at ~110 kyr BP. The best analog for the most extreme highstand at ~135 kyr BP is the highstand during the Early Holocene humid period from 10 to 6 kyr BP. The environmental conditions as reconstructed from diatom assemblages suggest long-lasting episodes of increased humidity during the high lake periods. This contrasts to the modern situation with a relatively shallow Lake Naivasha characterized by rapid water level fluctuations within a few decades. The most likely cause for the variable hydrological conditions since 175 kyr BP is orbitally driven insolation changes on the equator and increased lateral moisture transport from the ocean.

Keywords: East Africa; Diatoms; Transfer functions; Lake level; Paleoclimate; Pleistocene

---

1. Introduction

Diatoms are very sensitive indicators of various environmental parameters in a lake, such as water depth, chemistry, turbidity and nutrient supply (Gasse et al., 1995). Typical assemblages of these algae have been intensely studied in modern lakes, and also from cores and dry surface outcrops of paleolake sediments all over the world (Taub, 1996; Bradley, 1999; Battarbee, 2000; Gasse, 2000; Owen, 2002). Diatomite as sediment, comprising mainly fossil diatom skeletons, is a good archive of the conditions in a lake through time (e.g., Smol et al., 2001). Because changes of these conditions are mainly linked to climate, diatom assemblages provide indirect insights into the changes of the precipitation–evaporation balance in a catchment. A quantitative estimate of

---

* Corresponding author.
E-mail address: bergner@geo.uni-potsdam.de (A.G.N. Bergner).

0031-0182/$ - see front matter © 2004 Elsevier B.V. All rights reserved.
doi:10.1016/j.palaeo.2004.07.033

the environmental conditions through time is gained using diatom transfer functions (Gasse et al., 1995). Although reworking of diatom frustules, selective dissolution of some diatom taxa, and diagenetic alteration of the biogenic silica after deposition can cause significant distortions of the paleoenvironmental signal, cross-validation of the environmental reconstructions based on diatom assemblages with other proxies emphasizes the validity of the method (Gasse et al., 1997).

In the Central Kenya Rift, diatoms have been studied for a long time to reconstruct environmental changes in lake basins and hence climate changes on a variety of time scales (i.e., Nilsson, 1931; Richardson and Richardson, 1972; Richardson and Dussinger, 1986; Trauth et al., 2001). As identified in Late Pleistocene and Holocene deposits of Lake Naivasha, diatom-based paleohydrological reconstructions allowed to manifest periods of high water levels and low salinity at around 135, 110, 80 and 9 kyr BP (Richardson and Dussinger, 1986; Trauth et al., 2003). The precipitation–evaporation ratio during the most extreme highstands at ~9 and ~135 kyr BP has been determined using a lake-balance model, suggesting a minimum long-term increase in precipitation of about 30% (Bergner et al., 2003). However, the short-term trends and fluctuations as well as the amplitude of hydrochemical fluctuations on time scales on decadal to millennial time scales have not been investigated. We therefore studied the diatom assemblages contained in three diatomite deposits exposed in the Ol Njorowa Gorge south of the present lake. Using diatom transfer functions, we compared three highstands at ~135, ~110 and ~80 kyr BP with both the well-established highstand between 10 and 6 kyr BP (Richardson and Richardson, 1972; Washbourn-Kamau, 1975; Richardson and Dussinger, 1986) and the modern conditions in the lake. The results provide valuable insights into the natural variability of the lake system and its response to regional and global climate change.

2. Setting

Located at 1890 m above sea level, Lake Naivasha is the highest water body in the Central Kenya Rift (0°55′ S 36°20′ E; Figs. 1 and 2). The tectonically initiated lake basin is bounded by rift escarpments to the east and west, Mt. Eburru volcano to the north and Mt. Longonot volcano and the Olkaria Volcanic Complex to the south. The history of the Naivasha basin began at about 320 kyr BP, when Olkaria lava flows closed the basin to the south between the flanks of the 400-kyr-old Mt. Longonot and the escarpment to the west (Clarke et al., 1990; Fig. 2). These effusive bodies are unconformably overlain by an up to 60-m-thick fluvio-lacustrine sequence, between 175 and 60 kyr old, suggesting that the basin was covered by a lake three times larger than modern Lake Naivasha (Trauth et al., 2001, 2003; Bergner et al., 2003). After the regression of this lake in the Late Pleistocene, ongoing volcanic activity in the Olkaria Complex produced most of the present relief covering the older lake deposits (Clarke et al., 1990). After the formation of the Ol Njorowa Gorge by headward erosion of the outlet of the Early Holocene highstand, the Late Pleistocene sediments became exposed (Washbourn-Kamau, 1977). Today, the sediments are laterally continuous over a distance of more than 7 km and can be sampled in excellent dry sample outcrops of the gorges walls.

The modern Lake Naivasha is unique among the other lakes in the Central Kenya Rift because of its relatively low pH (~7.9) and electric conductivity (~250 and 500 $\mu S \cdot cm^{-1}$; Gasse et al., 1995; Verschuren, 1999). The freshness of the lake can be attributed to a significant groundwater seepage through permeable volcanic subsurface rocks and to the perennial freshwater supply from the Malewa and Gilgil rivers (Ojiambo and Lyons, 1996; Verschuren, 1999). The two streams drain a ~3200 km^2 large catchment area, which includes moist mountain ranges of the eastern (2200 to 2500 m a.s.l.) and western escarpments (up to 4400 m elevation). Whereas annual rainfall exceeds 1750 $mm \cdot year^{-1}$ in these regions, the fairly plain and wind-stressed Lake Naivasha basin is characterized by a negative moisture budget with rainfall averaging ~650 $mm \cdot year^{-1}$ and evaporation of ~1900 $mm \cdot year^{-1}$ (Jätzold, 1981; Kenya Meteorological Department, 2000).

Temporal variations in the hydrological budget of Lake Naivasha are mainly controlled by changes in precipitation, which is in turn linked to the seasonal migration of equatorial convergence zones, i.e., the

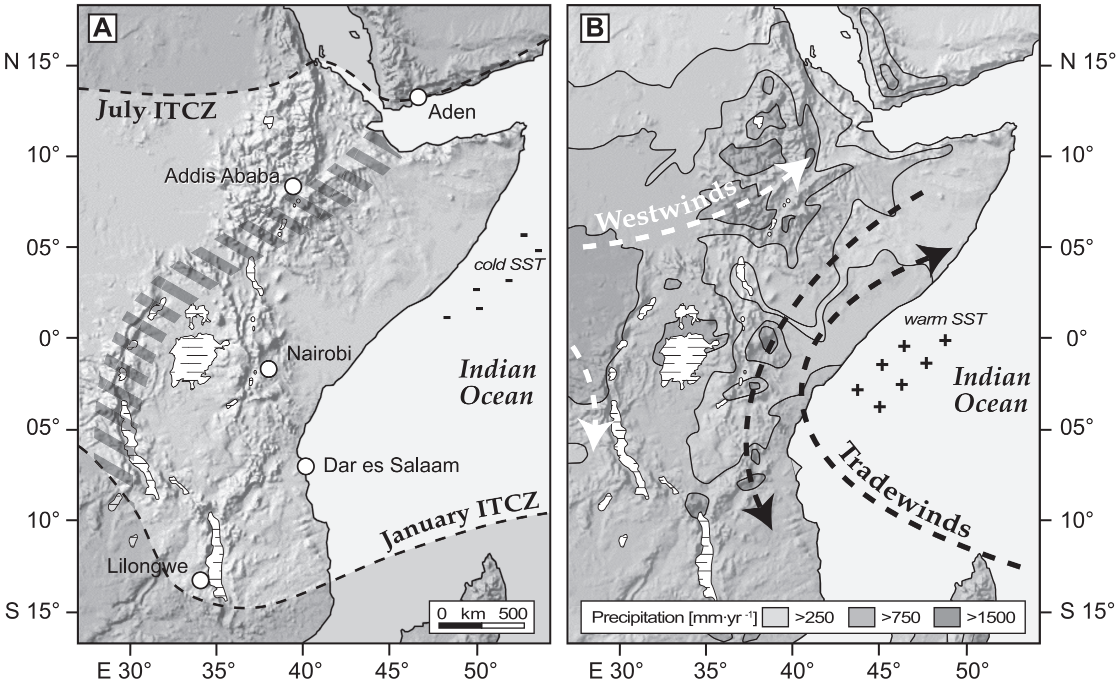

Fig. 1. Regional settings of the study area; (A) topography and location of large lakes; migration of Intertropical Convergence Zone (ITCZ, maximum position of July and January indicated) and Congo Air Boundary (CAB, dashed corridor) cause bimodal precipitation pattern with rainy seasons in April/ May (long rains) and October/November (short rains). (1) Lake Turkana, (2) Lakes Magadi and Natron, (3) Lake Eyasi, (4) Lake Victoria, (5) Lake Albert, (6) Lake Tanganyika, (7) Lake Malawi. (B) Airflow pattern of the study area changing significantly after transition of the ITCZ and CAB with predominant westwind streams from the Congo basin and trade winds from Indian Ocean (indicated by arrows). Shaded areas refer to regions with high precipitation as indicated. Symbols symbolizing sea-surface temperature anomalies in the Indian Ocean refer to higher moisture availability during El Niño events.

Intertropical Convergence Zone (ITCZ) and the Congo Air Boundary (Nicholson, 1996). Although heaviest rainfall occurs during April–May and October–November after the transition of the ITCZ, prevailing SE trade winds and westerly winds during summer, as well as NE trade winds and northwesterly air flow during winter cause minor rainfall in the Naivasha basin (Fig. 1). The short-term variability in the intensity of these wind systems is directly related to sea-surface temperature (SST) variations in the Indian, Pacific and Atlantic Oceans (Camberlin, 1995; Saji et al., 1999). In particular, the El Niño/Southern Oscillation (ENSO) accounts for a significant part of hydrological fluctuations on decadal time scales (Camberlin, 1995; Nicholson, 1996; Indeje et al., 2000).

As a consequence of these variations, the lake level is subjected to significant changes, which particularly affect the shallow areas of the lake (Gaudet and Melack, 1981; Tarras-Wahlberg et al., 2002). Geobiochemical processes in the nearshore parts of the lake account for much of the ionic removal and therefore may provide further explanation for the low alkalinity of the lake (Gaudet and Melack, 1981). The modern hydrochemistry of Lake Naivasha is classified as low-chloride, high-fluoride, sodium-bicarbonate water, where the acquisition of solutes by weathering of the surrounding feldspathoidic bedrocks masks the chemical composition of the rain (Gaudet and Melack, 1981; Tarras-Wahlberg et al., 2002). Due to the heavy afternoon winds and the shallow bathymetry, the water body of Lake Naivasha is polymictic and not thermally stratified (Verschuren, 1999). The intense mixing of the water column is also reflected in the modern diatom assemblages, collected from both, sediment and surface-water (i.e., plankton) samples. Herein, the typical modern diatom flora is dominated by *Aulacoseira ambigua*, *Aulacoseira granulata* var.

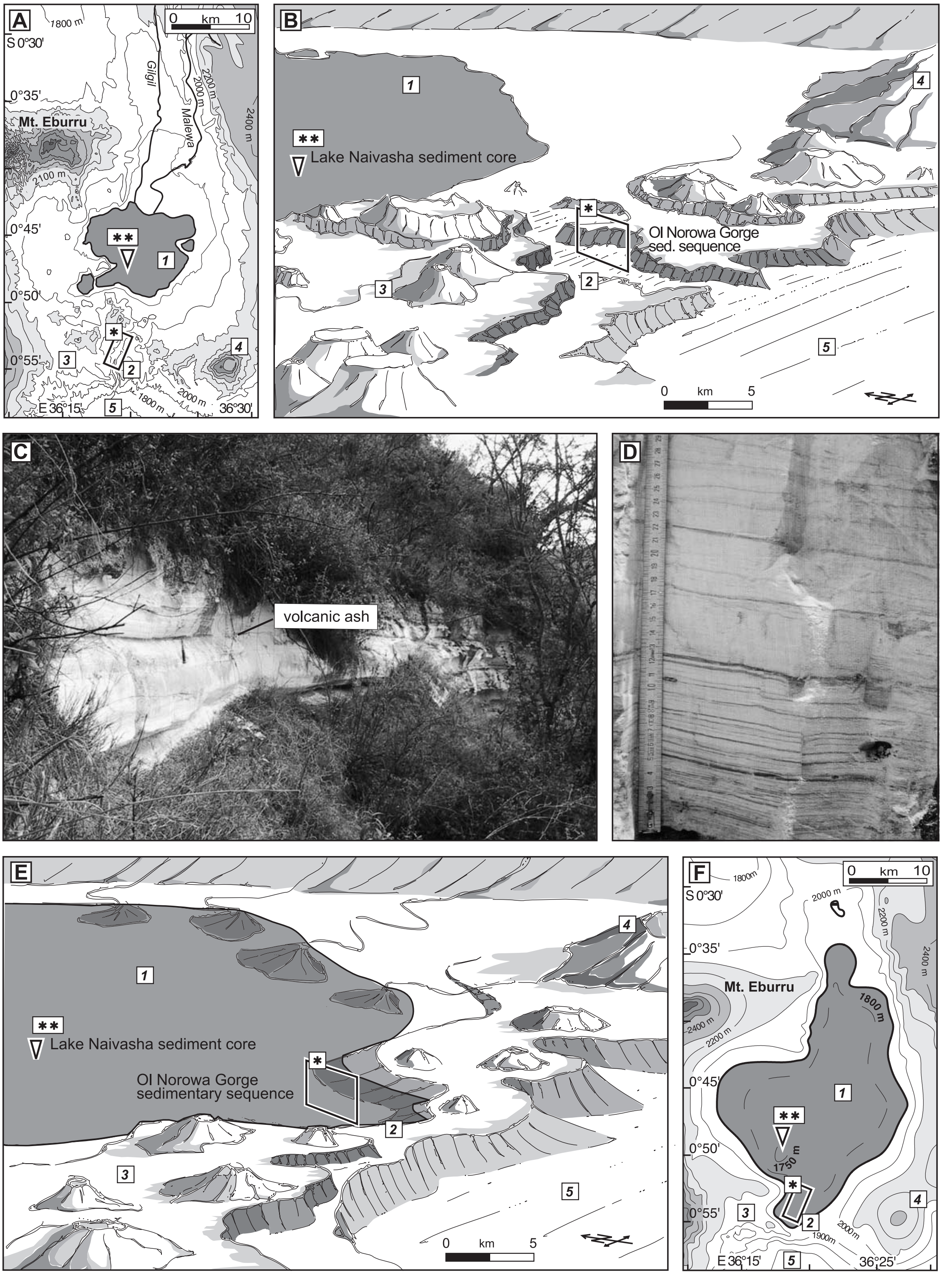
A
0 km 10
1800 m
S 0°30'
0°35'
Gilgil
Malewa
2200 m
2000 m
2400 m
Mt. Eburru
2100 m
0°45'
**
1
0°50'
*
2
3
4
0°55'
E 36°15'
5
1800 m
2000 m
36°30'
B
1
**
Lake Naivasha sediment core
4
*
Ol Norowa Gorge
sed. sequence
2
3
5
0 km 5
C
volcanic ash
D
E
4
1
**
Lake Naivasha sediment core
*
Ol Norowa Gorge
sedimentary sequence
2
3
5
0 km 5
F
0 km 10
1800m
S 0°30'
2000 m
2200 m
0°35'
2400 m
Mt. Eburru
1800 m
2400 m
2200 m
0°45'
1
**
0°50'
1750 m
*
4
0°55'
3
2
1900m
2000m
E 36°15'
5
36°25'

angustissima and *Synedra acus* (Richardson and Dussinger, 1986; Gaudet and Melack, 1981; Gasse et al., 1995).

3. Methods

According to an earlier composite chronology, the diatomite beds of the Ol Njorowa Gorge, south of modern Lake Naivasha, represent marginal deposits of three high lakes between 175 and 60 kyr BP (Trauth et al., 2001; Bergner et al., 2003; Fig. 2A and B). Based on 17 single-crystal ^{40}Ar/^{39}Ar-age determinations on intercalated tuff layers, the oldest diatomites, 340 and 120 cm thick, were accumulated during highstands IX (~135 kyr BP) and VIII (~110 kyr BP), whereas the youngest diatomite, up to 50 cm thick, records highstand V (~80 kyr BP; Trauth and Strecker, 1996; Trauth et al., 2003). We resampled the most prominent profiles of these deposits for a high-resolution microfossil analyses (cf. locations at Fig. 2C–F).

Depending on the quality of the sediment, we sampled at 10- to 30-cm intervals for highstand IX and VIII, and at 2.5-cm intervals for highstand V. In order to average potential seasonal variations in the species assemblages, we integrated 2.5-cm-thick slices of sediment for the investigation of the long-term trends. The dry sample material was washed in distilled water, organic matter was oxidized by H_2O_2 and carbonates were removed using HCl. Diatom slides were mounted in Naphrax and analyzed using a Leica optical microscope at magnification ×1000. Because of the limited preservation of the diatoms, we counted between 300 and 1000 valves per sample. We also estimated the content of detrital material and the percentage of broken valves for each sample relative to the total sum of counted valves. Furthermore, we documented the occurrence of phytoliths and sponge spicules as indicators of nearshore deposition. The ratio of broken diatoms, the amount of clastic debris as well as the phytolith content were regarded as a proxy for littoral conditions of the sampling site (e.g., Barker et al., 1990; Gasse et al., 1997). Because several sections of the profiles show strong laminations, high-resolution sampling and separate analysis were investigated in a 15-cm-thick continuous slice of diatomite to distinguish between the thin dark brown and thicker white laminae.

The diatom identification followed the principles of Hustedt (1949), Gasse (1986) and Krammer and Lange-Bertalot (1991a,b, 1997a,b). For paleohydrological and environmental interpretations, the identified taxa were cross-checked with the species listed in the modern East African Diatom Database, where both taxa counts and environmental variables of the sampling site are included (Gasse et al., 1995). Using this database, diatom-inferred conductivity, pH, cation and anion ratios were derived by transfer functions. Secondly, principle-component analysis (PCA) and hierarchical cluster analysis (CA) were used to identify groups of diatoms with comparable chemical and habitat characteristics. The routine *pca* of the Matlab® PLS_Toolbox provided by Eigenvector Research, Manson, was used to perform PCA on the auto-scaled data, implying all variables were put on an equal basis in the analysis (Swan and Sandilands, 1995; Wise et al., 2002). This was important because the ecological parameters of the diatoms show large differences in the absolute values of mean and variance. Next, we employed the Matlab® routine *cluster* on the auto-scaled data to define groups of diatoms with similar environmental preferences.

Fig. 2. (A) Map of the Naivasha basin showing present-day topography, extension of modern Lake Naivasha, main rivers, location of surface outcrops in the Ol Njorowa Gorge (square indicated by *) and sediment core from lake (triangle indicated by **; Richardson and Dussinger, 1986). (B) Present-day relief and lake area obtained from digital-elevation modeling. The idealized landscape ignores vegetation coverage, but shows the southern rim of the Naivasha basin as seen towards NE with (1) Lake Naivasha, (2) NNE–SSW orientated Ol Njorowa Gorge, volcanic complexes of (3) Olkaria and (4) Longonot, as well as (5) Akira plains. Location of sediment sequence in the Ol Njorowa Gorge (*) and sediment core profile from Lake Naivasha (**). (C) 3.40 m of diatomite surface outcrop in the Ol Njorowa Gorge, showing intercalated tephra (hammer for scale) and (D) laminated sections of higher detrital contents. Reconstruction of maximum extension of paleo-Lake Naivasha, as inferred from the results of this study and reconstruction of the bathymetry based on geologic field data (Bergner et al., 2003) showing (E) relief-sketch of the southern rim of the paleobasin derived from digital-elevation modeling outlining the extension of the paleo-Lake Naivasha and spatial relation of the sediment profiles and (F) estimated topography of the Naivasha basin with 100-m-contour interval; 1900 m a.s.l. corresponds to maximum lake level at ~135 kyr BP. Labeling corresponding to (A) and (B).

4. Results

4.1. Litho-/biofacies correlation

The diatomite beds of the Ol Njorowa Gorge consist by almost 100% of intact or variably fragmented diatom valves. Phytoliths and sponge spicules appear in subordinate numbers, i.e., less than 1% of the total number of counted particles. Glass shards and siliciclastic material are more frequent, but are generally restricted to the dark layers within the diatomite beds. The quality of the laminations within the diatomites was found to be an appropriate classification scheme to link macroscopic characteristics to the microscopic character of the sediments. Consequently, the diatomite beds can be classified into three lithologic facies: (a) pure-white diatomite with weak lamination, (b) diatomite with distinct lamination and (c) grayish diatomite with a relatively high clastic component, but without clear lamination. Microscopic inspection of the sediment character and preservation of diatom valves support our macroscopic classification scheme: The preservation of the diatoms is inversely correlated with the numbers of phytoliths and sponge spicules as well as the clastic particles (Fig. 3). Although the laminated sections show large internal variation in these parameters, they contain predominantly well-preserved diatom valves and minor amounts of phytoliths, sponge spicules and clastic debris. Within the nonlaminated sections, this pattern is reversed; significant amounts of broken valves occur more frequently, while high numbers of clastic debris, phytoliths and sponge spicules are more abundant. Assuming that clastic contaminations, phytoliths, sponge spicules and broken valves record more turbulent, nearshore sedimentary conditions, whereas intact diatom valves and the absence of phytoliths and sponges indicate calm, deep-water environments (Hecky and Kilham, 1973; Smol et al., 2001), we can use our classification of diatomites to estimate water depth and distance to the lake shore (Fig. 3). In the following, we apply this approach to the full thickness of the diatomites as well as to sections on lamination scale.

A first-order estimate for the hydro-ecological changes in the lake can be best illustrated by the ratio of planktonic vs. littoral species. Taking into account the relative importance of facultative–planktonic diatoms as deep-water indicators in littoral habitats, we recalculated the planktonic–littoral ratio by including the facultative–planktonic taxa in the plankton group (Fig. 3). Done for each highstand separately, the parameters nicely correlate with the changes in the lithologic facies as outlined above. Highstand IX is composed of four stratigraphic zones (Figs. 3 and 4): The lowest part of the diatomite extending from the base to 105 cm, comprises littoral diatoms, such as *Epithemia adnata*, *Epithemia sorex*, *Gomphonema intricatum* and *Cymbella cistula*, but the assemblage is clearly dominated by facultative–planktonic species, such as *Fragilaria pinnata* and *F. construens*. Deep-water indicators, such as *Aulacoseira granulata*, *Cyclotella ocellata*, *Cyclotella glomerata* and *Nitzschia tropica* are rare and only increase slightly in the uppermost section. Within the less or nonlaminated zone 2 (105 to 180 cm), the portion of the facultative–planktonic *Fragilaria* spp. is reduced, whereas periphytic *Cocconeis placentula*, *E. sorex*, *G. intricatum* and *Mostogloia elliptica* become more frequent. Zone 3 (180 to 250 cm) is again laminated and characterized by predominant planktonic species, mainly of *Aulacoseira* spp. and *Cyclotella* spp. In the uppermost, siltic and nonlaminated part of the diatomite, again more nearshore, littoral taxa prevail, predominated by facultative–planktonic *Fragilaria* spp. and a higher fraction of periphytic *E. adnata*, *Cymbella muellerii*, and *Gomphonema gracile* (Fig. 4A).

A similar, but much less distinct trend is observed in the diatomite profile of highstand VIII (Figs. 3, 4B): Planktonic species, like *Aulacoseira granulata* or *Nitzschia vanoyei*, and facultative–planktonic diatoms, such as *Cyclotella stelligera* and *Synedra ulna*, are concentrated in the lower, more laminated section of the profile (zone 1). The maximum in the planktonic–littoral ratio occurs at around 30 cm above the diatomite base, corresponding to a decrease in the occurrence of phytoliths and sponge spicules. In this section, also the preservation of the diatom frustules is good, and only minor amounts of clastic debris are observed. In the upper part of the profile, where this dominance of littoral genera, such as *Fragilaria*, *Gomphonema* and *Epithemia* gets striking, the content of clastic debris as well as the number of phytoliths and sponge spicules increases. Herein, the

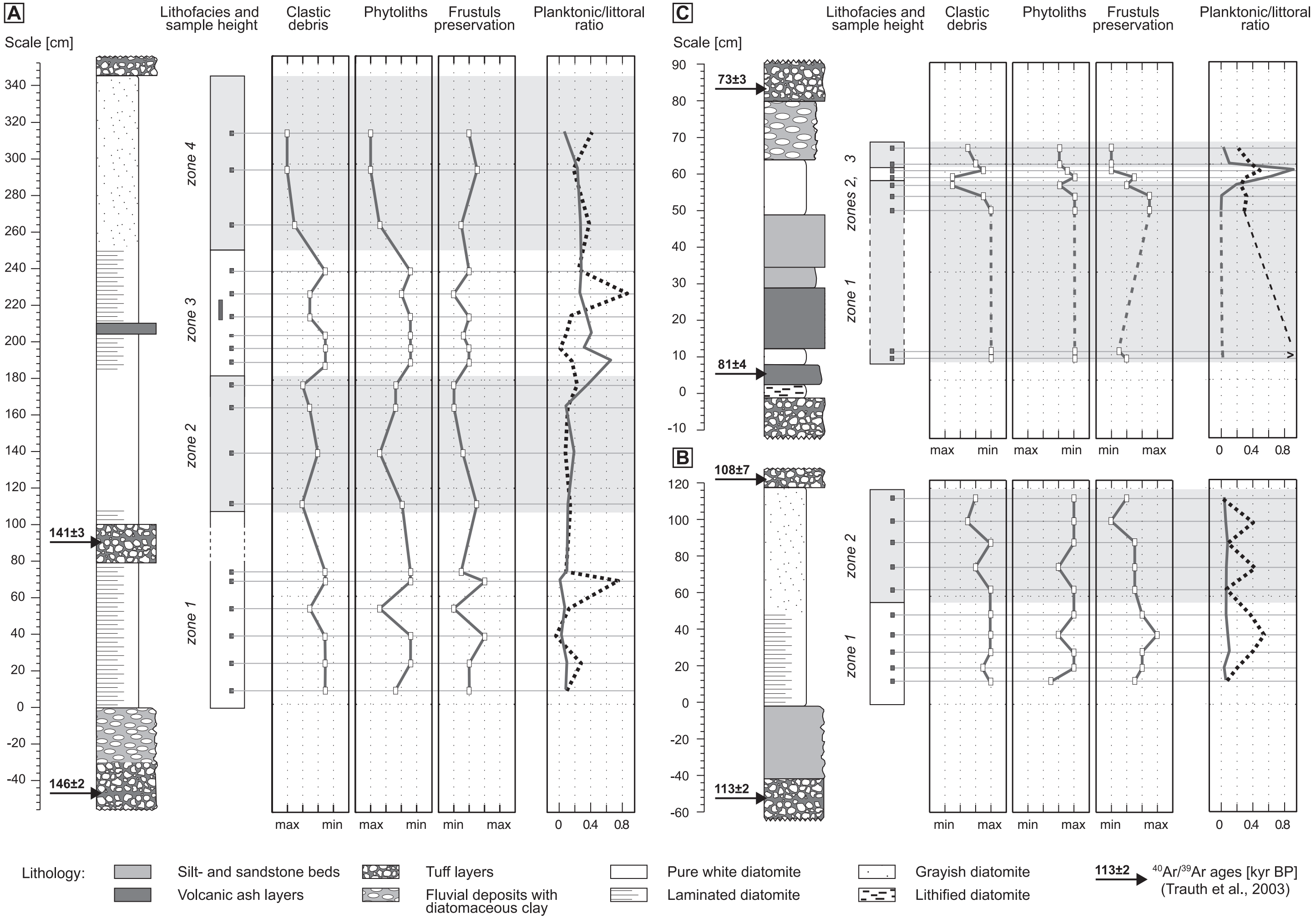

Fig. 3. Lithostratigrapic profiles of diatomites of (A) highstand IX (146±2 to ~120 kyr BP), (B) highstand VIII (113±2 to 108±7 kyr BP) and (C) diatomites and diatomaceous silts of highstand V (81±4 to 73±3 kyr BP). Age control from ^{40}Ar/^{39}Ar dating on sanidine phenochrysts from intercalated volcanic tuff beds (Trauth et al., 2001, 2003). Semiquantitative plots of sedimentological parameters obtained from thin-section analysis. Planktonic–littoral ratio of diatom taxa reflecting the fraction of planktonic vs. periphytic and facultative–planktonic diatoms (solid line), and planktonic, including facultative–planktonic vs. periphytic diatoms (dashed) within the identified diatom assemblages. Environmental information corresponds to the data set of East African diatoms (Gasse et al., 1995).

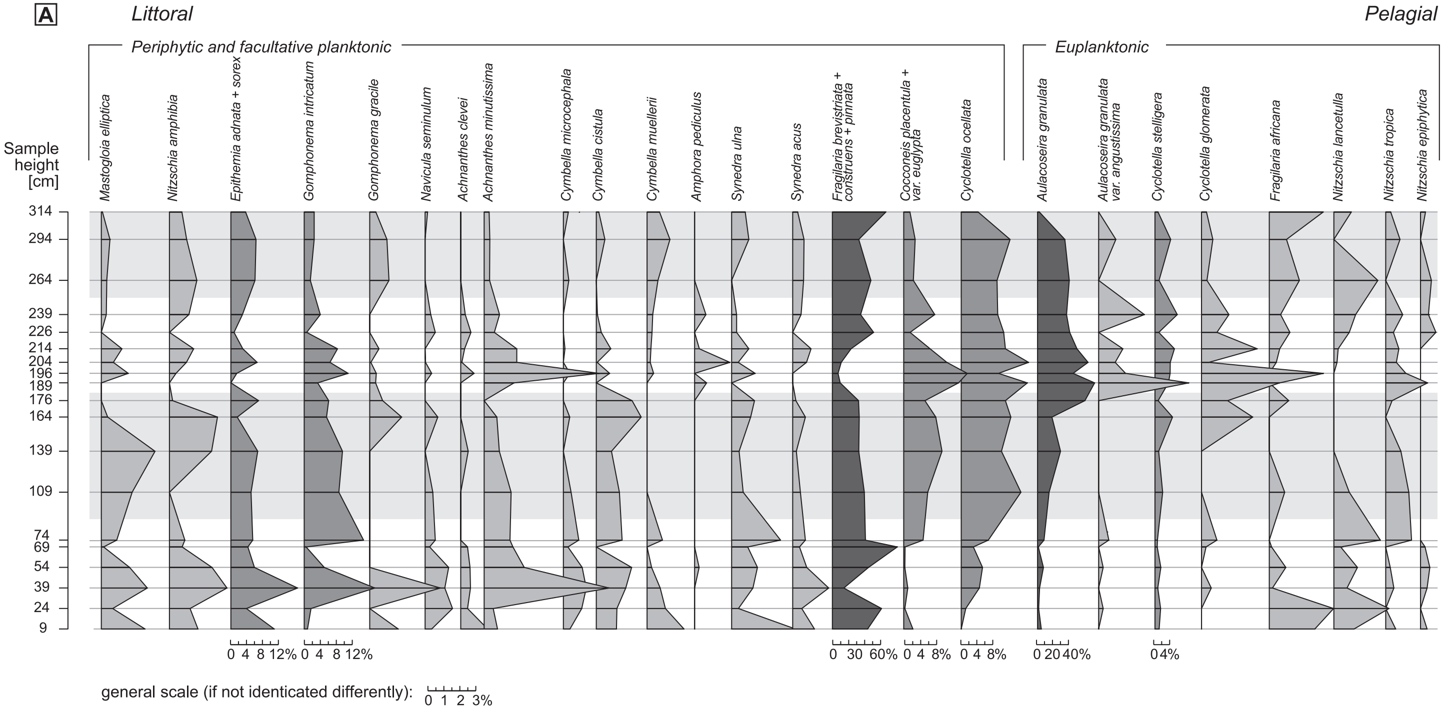

Fig. 4. Relative abundance of selected diatom species in profiles of (A) highstand IX, (B) highstand VIII and (C) highstand V. Shadings correspond to sediment facies (cf. Fig. 3).

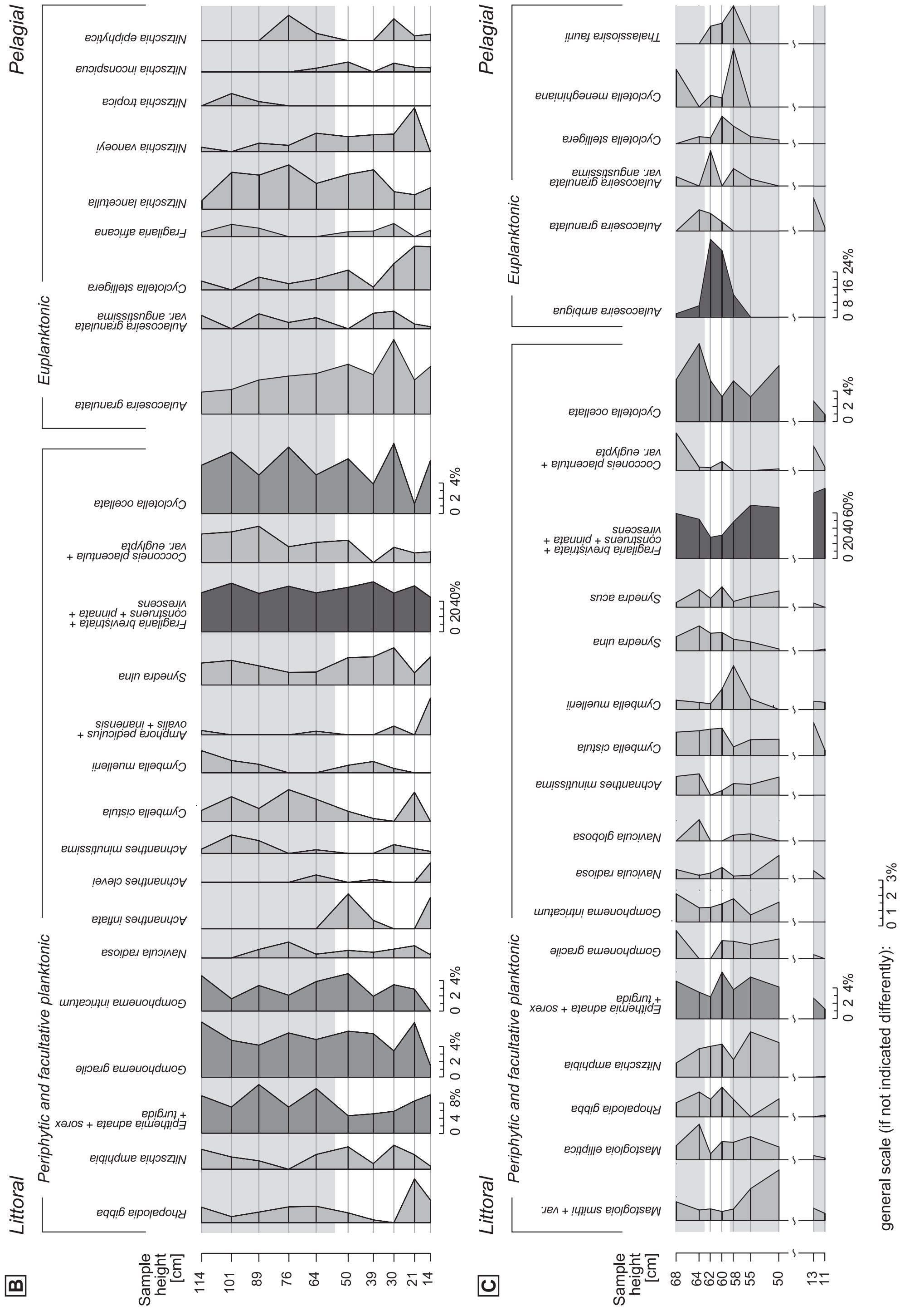

Fig. 4 (*continued*).

fraction of planktonic diatoms is low and never exceeds 8%.

Although the diatomaceous beds of highstand V do not show any laminations, even these units show similarities between sediment facies and the relative abundance of diatom taxa (Figs. 3 and 4B). Throughout the profile, periphytic and facultative–planktonic diatoms predominate in the diatom assemblages. Only within a distinctive, narrow zone between 58 and 64 cm above the base of the diatomite (zone 2), an abrupt increase in planktonic, freshwater diatoms of *Aulacoseira ambigua* (up to 40%), accompanied by abundant *Aulacoseira granulata* and *Cyclotella stelligera*, is observed. Interestingly, the amount of clastic debris is significantly reduced and phytoliths and sponge spicules occur more seldom in this section.

In order to fully understand the relationship between the occurrence of clastic materials and the biological inventory, a short section of the well-laminated highstand-IX diatomite (212 to 225 cm above its base) was analyzed in 0.25-cm intervals and from thin sections. The comparison of the species assemblages within pure-white and brownish clay-rich layers indicates a clear anticorrelation between the amount of clastic material and the number of planktonic diatoms. Moreover, decreasing numbers of phytoliths and sponge spicules correlate with higher amounts of well-preserved diatom frustules and a predominance of planktonic genera in the diatom assemblages (Fig. 5). From thin section analysis, it can also be concluded that clay-rich, dark layers do not document annual or seasonal layers, but most likely reflect repeated events of higher clastic input. Such features can best be explained by rhythmic deposition of suspended material, which is initiated by enhanced sediment input or turbulences in the littoral lake areas (Wetzel, 2001). Both processes would account for a reworking of loose sediment, an increased transport of littoral deposits towards deeper parts of the lake and hence enhanced mixing of planktonic and littoral diatom fragments. Additionally, bioturbation may disturb the original laminated texture of lake sediments. Benthic oxygenation and nutrient supply are the key parameters influencing the intensity of benthic mixing in aquatic environments (Robbins et al., 1977; Battarbee et al., 2001). Although these is some evidence for tracks and burrows in some parts of the diatomites, bioturbation was obviously not intense enough to completely destroy the layering of the sediments. The presence of laminae therefore suggests limited oxygen and nutrient supply during deeper-water conditions, whereas the absence of laminate documents shallow-water nearshore environments. Similar observations were described in comparable deposits of East African lakes (e.g., Roberts et al., 1993; Damnati and Taieb, 1995; Gasse and Van Campo, 2001).

Although the understanding of the internal dynamics of the lake system would require a more detailed investigation of the laminated part of the section, these preliminary results help to interpret the observed long-term trends in the diatom flora. As reflected in the planktonic–littoral ratio, all highstands are characterized by long-term trends from more littoral, shallow-water conditions to deeper freshwater environments. This trend is overlain by short-term fluctuations, as indicated by the highly varying sedimentological and paleontological parameters in the laminated sections of the profile. In these sections, littoral, i.e., periphytic and facultative–planktonic species get more abundant where brownish silt layers alternate with pure-white diatomite. The relative importance of littoral taxa inversely correlates with the thickness of the white layers, as it can best be studied in the laminated, basal part of the highstand-VIII diatomite (Fig. 2D).

While interpreting the results from this analysis, it has to be kept in mind, that the fossil flora may represent an only incomplete picture of the original assemblage. The limited preservation of at least some of the samples suggests that this factor could be of some relevance in the Ol Njorowa Gorge sequence. Above all, breaking of larger *Navicula*, *Pinnularia* or *Synedra* frustules is a problem throughout the sequences and thin-walled frustules are less abundant than morphologically stronger diatoms. The treatment of the dry sample material for diatom slides may have also affected fragile skeletons. However, the comparison of diatom slides with smear slides and thin sections yields no significant difference in the preservation of the diatom frustules. Obviously, the damage of the valves has to be explained by sedimentary processes in the paleolakes. Because the location of the Ol Njorowa Gorge section is believed to represent the littoral part of a lake, reworking of diatom frustules may be of some importance (Gasse et al., 1997).

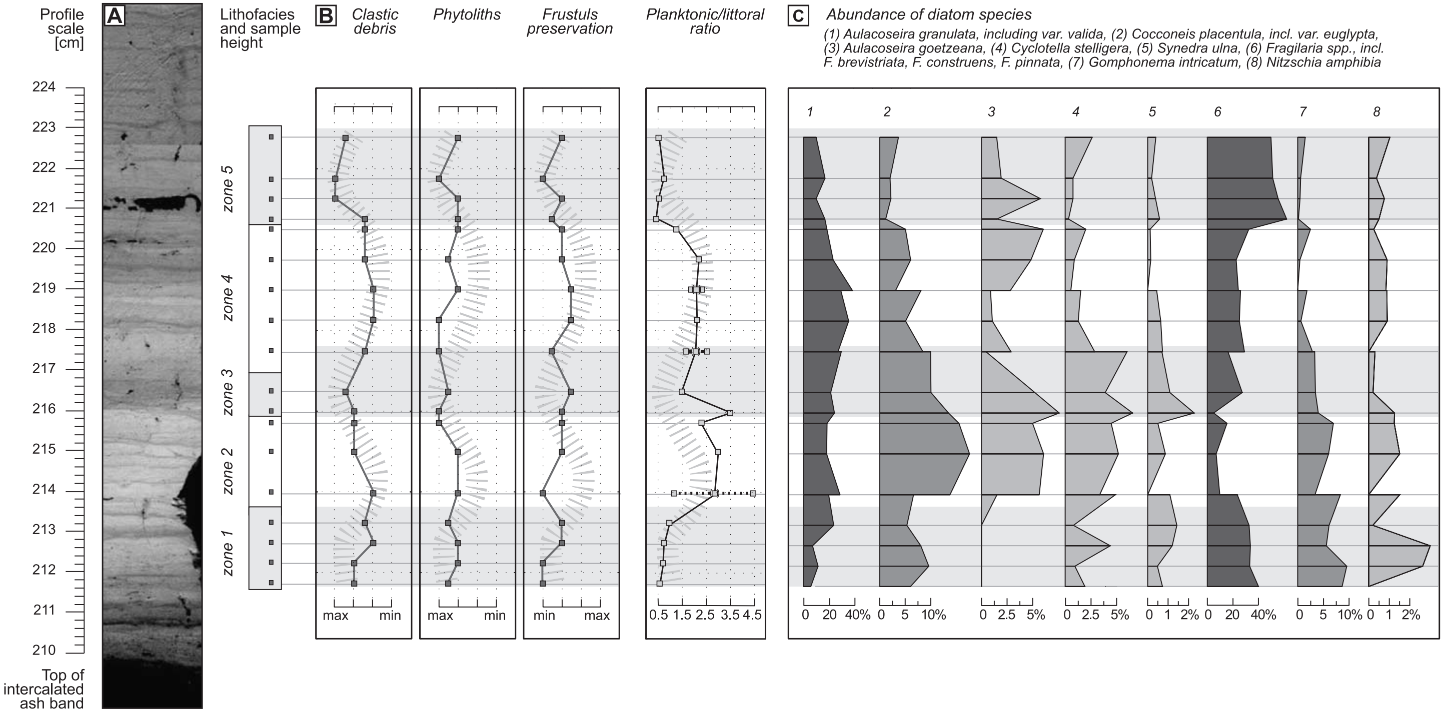

Fig. 5. Results of high-resolution analysis of laminated highstand-IX diatomite. (A) Investigated slice of diatomite shows strong laminations with alternating pure-white and brownish clay-rich layers. Analyses were performed in ~0.25-cm intervals, for comparison between the characteristics of the laminae and diatom assemblages. (B) Variance of sedimentological parameters and planktonic–littoral ratio. (C) Relative abundance of selected diatom species. Shadings correspond to facies of more dense vs. wider laminations; dashed line reflect overlain trend.

4.2. Estimation of paleoenvironmental parameters

After having determined the species assemblages and their temporal variations, we used this data matrix for the reconstruction of the hydrochemical trends during each highstand. The East African Diatom Database was utilized as a modern analog for the diatoms observed in our samples (Gasse et al., 1995). Applying multivariate transfer techniques, we calculated estimates of conductivity, pH, cation (Na^++K^+/Ca^{2+}+Mg^{2+}) and anion (CO_3^{2-}+HCO_3^-/Cl^-+SO_4^{2-}) ratios for each fossil sample. In order to separate various environmental influences on the evolution of the diatom assemblages and increase the signal-to-noise ratio of the data, principle-component analysis (PCA) and hierarchical cluster analysis (CA) have been used to identify groups of diatoms indicating similar chemical and habitat characteristics (Swan and Sandilands, 1995). Using the Mahalanobis distance of the graphical output of the CA, seven main groups were identified for a number of 102 diatom species. Only 15 species with no ecologic information and 7 species with incomplete ecologic information were excluded from the CA. Between 86% and 100% of the diatom species identified in the different stratigraphic levels are listed in the East African Diatom Database. The seven groups of diatoms as defined from CA can therefore be regarded as to be representative for the true flora of the paleolakes and can be used for our environmental reconstructions (Table 1).

Table 1
Results of diatom cluster analyses with calculated means of environmental parameters according to individual values from East African Diatom Dataset (Gasse et al., 1995)

Cluster	Number of diatom species	Means of			
		pH	Conductivity ($\mu S \cdot cm^{-1}$)	Cation ratio (log)	Anion ratio (log)
A	17	8.02	1900	0.53	−0.39
B	4	7.94	2200	0.38	−0.35
Mean (A+B)		7.98	2000	0.46	−0.37
C	21	7.99	850	0.30	0.02
D	20	7.84	300	0.30	0.29
E	14	7.49	200	0.18	0.56
F	4	7.26	150	−0.09	0.75
Mean (E+F)		7.37	180	0.05	0.67
G	7	9.24	13,800	1.58	−0.36

As a first step, arithmetic means of the pH, conductivity values, anion and cation ratios were calculated for each diatom cluster separately. Whereas groups A to F obviously reflect freshwater conditions with a preferred pH between 7.3 and 8.0, and conductivity values between 150 and ≤2000 $\mu S \cdot cm^{-1}$, only diatom species comprising cluster G prefer strongly saline–alkaline conditions with pH values of =9.0 and conductivity values above 5000 $\mu S \cdot cm^{-1}$. Taken into account the close similarities of groups A and B, and E and F, respectively, the clusters were merged to five fields of hydrochemical preference based on their pH and conductivity values (Table 1; Fig. 6A). Moreover, the genus *Fragilaria* was excluded from the clusters, because of its predominance in nearly all samples. After this pretreatment of the data, new graphs were created showing the occurrence of the diatoms for each cluster reflecting the hydrochemical conditions vs. depth (Figs. 6B–D and 7). These plots characterized by a higher signal-to-noise ratio now provide a much better base for the paleohydrological interpretation.

The variations in the importance of each diatom cluster through time nicely correlates with the sediment facies as described above as well as with the planktonic–littoral ratio (Fig. 7). In the lowest section of the profile of highstand IX (i.e., zone 1), the flora is clearly dominated by diatom taxa of clusters A, B and G preferring higher pH (=8.0) and elevated conductivity values (>400 $\mu S \cdot cm^{-1}$). Within zone 2, these diatom species with a saline–alkaline preference are replaced by taxa reflecting stabilizing freshwater conditions (clusters D, E and F). In the lithologic zone 3, between +180 and +250 cm, diatoms of a very low pH dominate the community, whereas saline–alkaliphilous species are almost absent. Between +200 and +260 cm, around ~50% of diatoms preferring a pH of ≤7.5 and abundant diatoms of intermediate pH and conductivity of <400 $\mu S \cdot cm^{-1}$ indicate that relatively stable freshwater conditions have been established over a relatively long period of time. Interestingly, *Fragilaria* spp. return to the diatom community at the end of zone 3, whereas similar alkaliphilous taxa never reach the high numbers as observed in the lower part of the profile (Fig. 7A).

As already indicated by the planktonic–littoral ratio, the diatom assemblages of highstand VIII are very different from highstand IX (Figs. 6C and 7B).

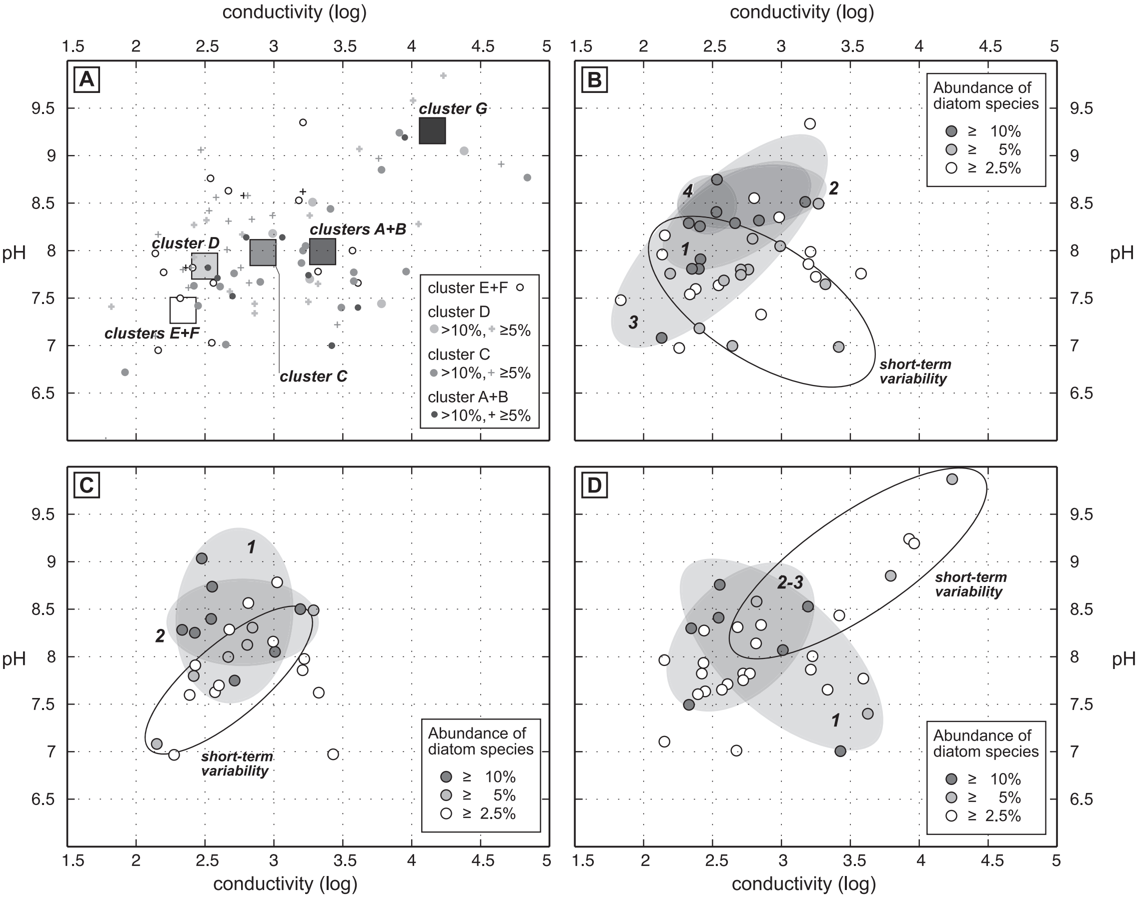

Fig. 6. Paleohydrology inferred from diatom assemblages. (A) Principle-component and hierarchical cluster analyses defining five groups of diatom species with distinctive hydrochemical preference. Large squares refer to calculated means (cf. Table 1), small symbols indicate individual values of single diatom species (cluster G not indicated). Temporal variation of hydrochemical conditions in the reconstructed paleolakes as derived from abundance of hydrochemical clusters for (B) highstand IX, (C) highstand VIII and (D) highstand V showing prevailing diatom species (circles) vs. time. Time slices correspond to sediment facies of profiles (cf. Fig. 3).

Throughout the profile, pH fluctuates around ~8.0 to ~8.5, whereas conductivity values vary between 300 and 1000 $\mu S \cdot cm^{-1}$. Diatoms preferring freshwater conditions with depleted pH (≤7.5), as represented by clusters E and F, never appear in greater numbers and only reach ~25% in zone 1. In contrast, alkaliphilous species appearing in zone 2, reflect increasing saline–alkaline conditions. Similar to highstand IX, also in this profile, the interval of optimal freshwater conditions correlates with the maximum planktonic–littoral ratio (at around 30 cm above the diatomite base; cf. Fig. 7B). In contrast to the previous highstands, diatom assemblages indicate prevailing saline–alkaline conditions with conductivity values of more =1000 to 3000 $\mu S \cdot cm^{-1}$ and pH up to 9.5 in large parts of the profile of highstand V (Figs. 6D and 7C). On the other hand, two distinct maxima in the occurrence of planktonic species suggest that also this highstand went through a period with deeper freshwater conditions (clusters E, F and G). The abrupt shift from alkaliphilous *Thalassiosira faurii* towards freshwater-preferring *Aulacoseira ambigua* emphasizes the rapid changes in hydrochemistry typical for this lake period.

Together with the results of the litho- and biofacies correlation, the diatomite deposits can be interpreted as reflecting the temporal evolution of three paleolake highstand periods with long-term stable, but individual hydrological characteristics.

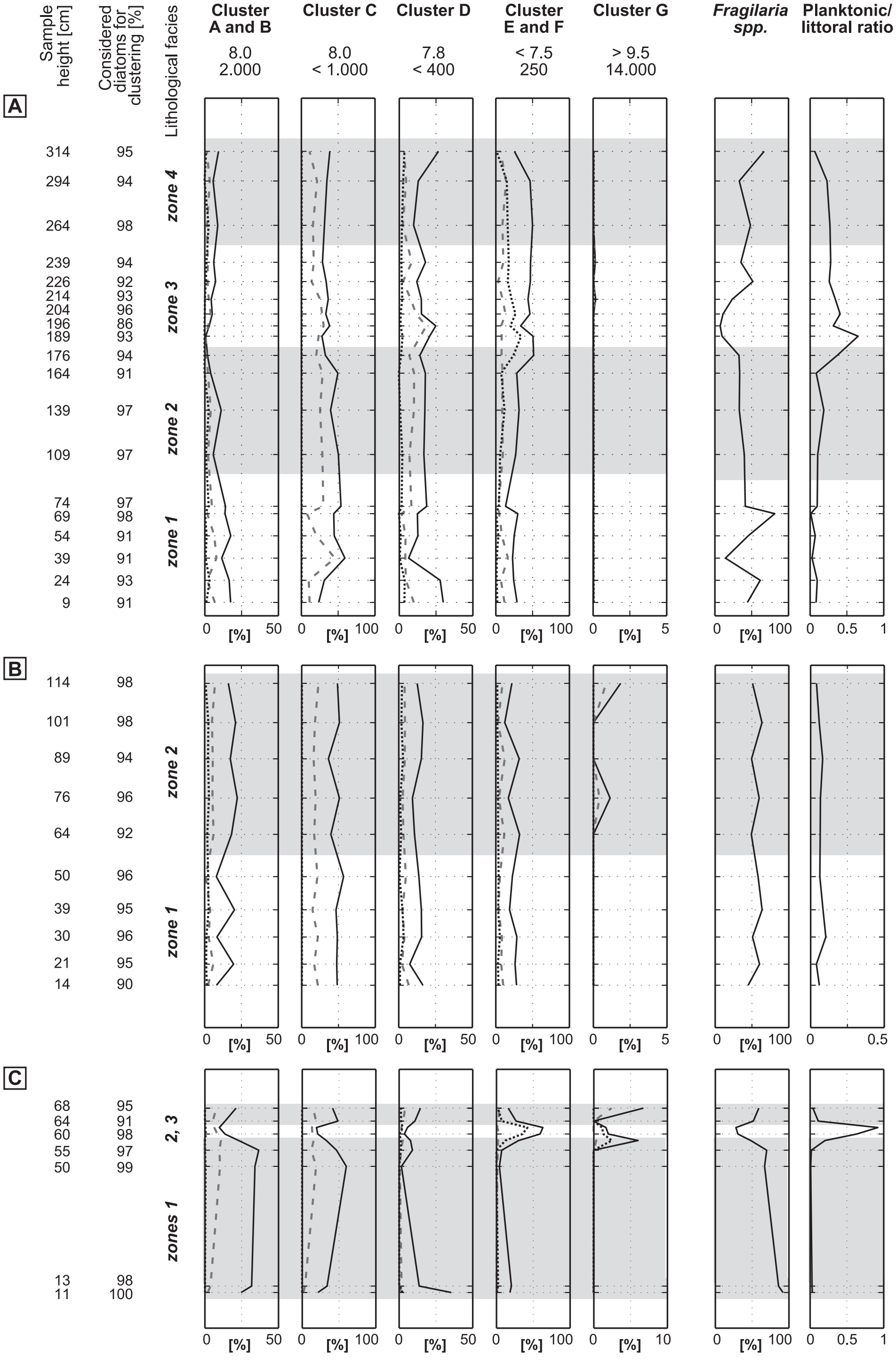

Fig. 7. Temporal variation of hydrochemical diatom clusters indicating total fraction of species belonging to one cluster (in %), fraction of littoral (dashed) and planktonic species (dotted) for (A) highstand IX, (B) highstand VIII and (C) highstand V. Fraction of nonconsidered *Fragilaria* spp. and plot of planktonic–littoral ratio for comparison. Shadings correspond to sediment facies of profiles (cf., Fig. 3).

Whereas the first highstand initiating after 146±2 kyr culminated in a deep lake with freshwater conditions and low alkalinity, the later highstands were shallower and characterized by increased pH and salinity. Interestingly, highstand IX went through a stage of clear dilution, corresponding to the peak in the planktonic–littoral ratio (zone 3 in Fig. 6B), whereas the deepest lake periods of highstands VIII and V (zones 2 in Fig. 6C and D) were characterized by more saline–alkaline conditions. These results furthermore emphasize that the peak in planktonic–littoral ratio gives a reliable approximation about the timing of the deepest lake stages.

Clearly, the lake deposits reflect the environmental conditions of the southernmost nearshore habitat of the paleolake. The observed disturbances of clastic layers are attributed to periodically rainfall events increasing the suspension of the lakes. Obviously, each lake period was initialized by several extreme flood events, which dramatically decreased both pH and conductivity and led to significant blooms of planktonic diatom populations. Laminae thicknesses increased with time, suggesting higher bioproductivity of constantly deepening lakes. After dilution, relatively stable freshwater conditions lasted for longer periods of time, before the lake levels declined and longer periods of low water levels and higher alkalinity occurred in the lake basin.

4.3. Temporal evolution of the highstands

A precise chronology for the evolution of the highstands is difficult to reconstruct due to the limited availability of radiometric age determinations and their uncertainties. The 0.8-m-thick section of the oldest diatomite (highstand IX) between the 146±2-kyr-old tuff at the base of the unit and the 141±3-kyr-old intercalated tuff has deposited within a time period of 5.0±3.6 kyr (one-sigma uncertainty according to the Gaussian law of errors). This estimate considers that no hiatus was observed from visual inspection of the sediments in the field or the analysis of the flora. The 1.2 m of diatomite of highstand VIII is bracketed by 113±2- and 108±7-kyr-old tuff layers, implying a hydrological evolution over a time span of about 5.0±7.2 kyr. The deposits of highstand V accumulated between 81±4 and 73±3 kyr BP, i.e., within approximately 8.0±5.0 kyr.

These numbers suggest average sedimentation rates for the diatomites between 0.03 and 0.25 mm/year. However, the maximum thickness of the laminae as observed in the thin slices is up to 10 mm. Unfortunately, the analysis of the laminated sections yields no detailed information about the mechanism causing the layering. As indicated by the lithological indicators, brownish layers record increased clastic influx, as possibly triggered by increased surface runoffs following high rainfalls. According to the hypothesis by Nilsson (1931) and Richardson and Richardson (1972), one or two couplets of white and brownish layers would correspond to 1 year of sedimentation. That would imply maximum sedimentation rates of 10 $\mathrm{mm \cdot year^{-1}}$ for large parts of the profiles, but sedimentation rates for diatomites are usually lower in most lakes (much less than 1 $\mathrm{mm \cdot year^{-1}}$; Richardson and Dussinger, 1986; Telford and Lamb, 1999; Stager and Johnson, 2000; Chalié and Gasse, 2002; D. Livingston, personal communication 2002). We suggest a more complex interpretation of the laminae, including a bimodal precipitation signal, which is modulated by a strong multiannual or decadal, ENSO-type influence. The hypothesis then proposes that the darker layers occurring every 3 to 7 years could be attributed to an El-Niño-like precipitation increase in the catchment area (see Fig. 2D; cf., Damnati and Taieb, 1995).

However, taken into account the uncertainties in $^{40}\mathrm{Ar}/^{39}\mathrm{Ar}$ dating and the interpretation of the laminae, the best estimate for the mean sedimentation rate is ~0.2 $\mathrm{mm \cdot year^{-1}}$. According to thick laminae in the laminated sections of the profiles, we propose higher rates of sediment accumulation during stabilized deep-water conditions, whereas the shallow-water episodes were characterized by low sedimentation rates. Similar observations are described as a common feature in comparable lake sediments of East Africa (cf. Richardson and Dussinger, 1986; Telford and Lamb, 1999; Stager and Johnson, 2000; D. Livingstone, personal communication 2002; Owen, 2002; Barker and Gasse, 2003). We therefore conclude that the highstand-IX paleolake lasted from the first manifestation of lacustrine conditions until its complete regression for about 7000 to 15,000 years, whereas highstand VIII persisted about 5000 years, but highstand V only 3000 years.

5. Paleoclimatic implications of the reconstructed highstand periods

The detailed analysis of three diatomite profiles exposed in the Ol Njorowa Gorge reveals the enormous hydrological variability of Lake Naivasha during the last 175 kyr. The most significant difference between the reconstructed paleolake highstands and modern Lake Naivasha is the relative stability of the hydrological conditions through time. Our results as well as data from investigations of a 15-m-long sediment core (Richardson and Dussinger, 1986) suggest that the lake experienced at least two major and two intermediate lake-level highstands during the last 175 kyr (Fig. 8). Diatom analyses reveal that the high lakes at ~135 and ~9 kyr BP were clearly dominated by abundant planktonic diatom species typical for deep freshwater lakes. The sediments of both highstands document the existence of high lake levels during a period of several thousand years. Beach pebbles and paleoshorelines as well as basin reconstructions indicate that Lake Naivasha was up to 150 m deeper than today at that time (Washbourn-Kamau, 1975; Bergner et al., 2003). Because the lake also contributed water to the northern Nakuru-Elmenteita basin and to the southern Akira plains at least during the highstand at ~9 kyr BP (Washbourn-Kamau, 1977; Dühnforth, 2001; Dühnforth et al., 2001), we conclude that Lake Naivasha at ~135 and ~9 kyr BP went through the most extreme hydrological conditions during the last 175 kyr.

Whereas the diatom assemblages during the 135- and 9-kyr highstands show great similarities, significant differences are observed between the flora of the 110-kyr and 80-kyr highstands. The 110-kyr highstand has no analog during the last 175 kyr, with respect to the diatom flora. In contrast, diatom assemblages of the 80-kyr highstand and the flora preserved in the modern sediment imply comparable environmental conditions during these periods. Diatom analyses on short sediment cores from the modern lake reflect a similar temporal trend in the evolution of diatom assemblages in the last 5000 years as during the 80-kyr highstand (Richardson and Dussinger, 1986). Starting from a predominantly alkaliphilous flora, the diatom assemblages develop toward a freshwater-preferring community. This similar pattern reflects a similar freshening of the lakes with time and comparable environmental conditions. On the other hand, the higher fraction of planktonic taxa during the 80-kyr highstand suggests a slightly deeper lake during the Late Pleistocene. From morphologic constraints, we furthermore believe that the 80-kyr paleolake was larger than the modern equivalent in the open-water area.

In contrast to all other lake periods when diatomite has been deposited, the 110-kyr highstand does not show a dominance of planktonic algae. The diatom flora much more reflects nearshore lake habitats, and also the reconstructed paleoenvironmental conditions suggest a freshwater swamp and not a deep lake. Although the hydrological conditions at ~110 kyr BP were different from those during the other highstands, the sedimentary facies is similar, but different from the modern deposits. Whereas the modern Lake Naivasha is characterized by permanent sediment mixing due to wind-driven resuspension (Verschuren, 1999), the laminated deposits of the paleolake imply wind-sheltered sedimentation in a (most probably) deeper lake environment. In that sense, the 110-kyr highstand can be regarded as an intermediate stage between the highest lake levels and the modern lowstand conditions.

Comparing our results with other lake-level records derived from several sediment cores in the Naivasha and Nakuru-Elmenteita basins, an interesting chronology of lake-level fluctuations can be compiled for the last 175 kyr (Fig. 8). Because important tectonic movements did not affect the Naivasha basin during that time, the hydrological changes are interpreted as to reflect variations in the precipitation–evaporation

Fig. 8. Correlation of lake-level changes of Lake Naivasha and orbitally induced changes of climatic parameters. (A) Contour plot of the anomalous heat flux ($\mathrm{W \cdot m^{-2}}$) onto the equator (contour interval is 20 $\mathrm{W \cdot m^{-2}}$, solid lines indicate values ≥ 400 $\mathrm{W \cdot m^{-2}}$). Seasons of prevailing airflow pattern indicated by horizontal bars (cf. Fig. 1); data from Berger and Loutre (1991). (B) Composite chronology of hydrologic changes in the Central Kenya Rift with age control points from this study ($^{40}\mathrm{Ar}/^{39}\mathrm{Ar}$ dated) and Richardson and Dussinger (1986) ($^{14}\mathrm{C}$ dated); shadings indicate most extreme lake-level highstands; solid bars refer to estimated highstand interval. (C) $\mathrm{U}_{37}^{\mathrm{K}}$-based Indian Ocean sea-surface temperatures (marine core MD85674; Bard et al., 1997); solid line according to tuning on SPECMAP time scale; dashed line according to timing of Termination II by Shackleton et al. (2003). (D) Vostok deuterium content of ice as a proxy for atmospheric temperature (Petit et al., 1999).

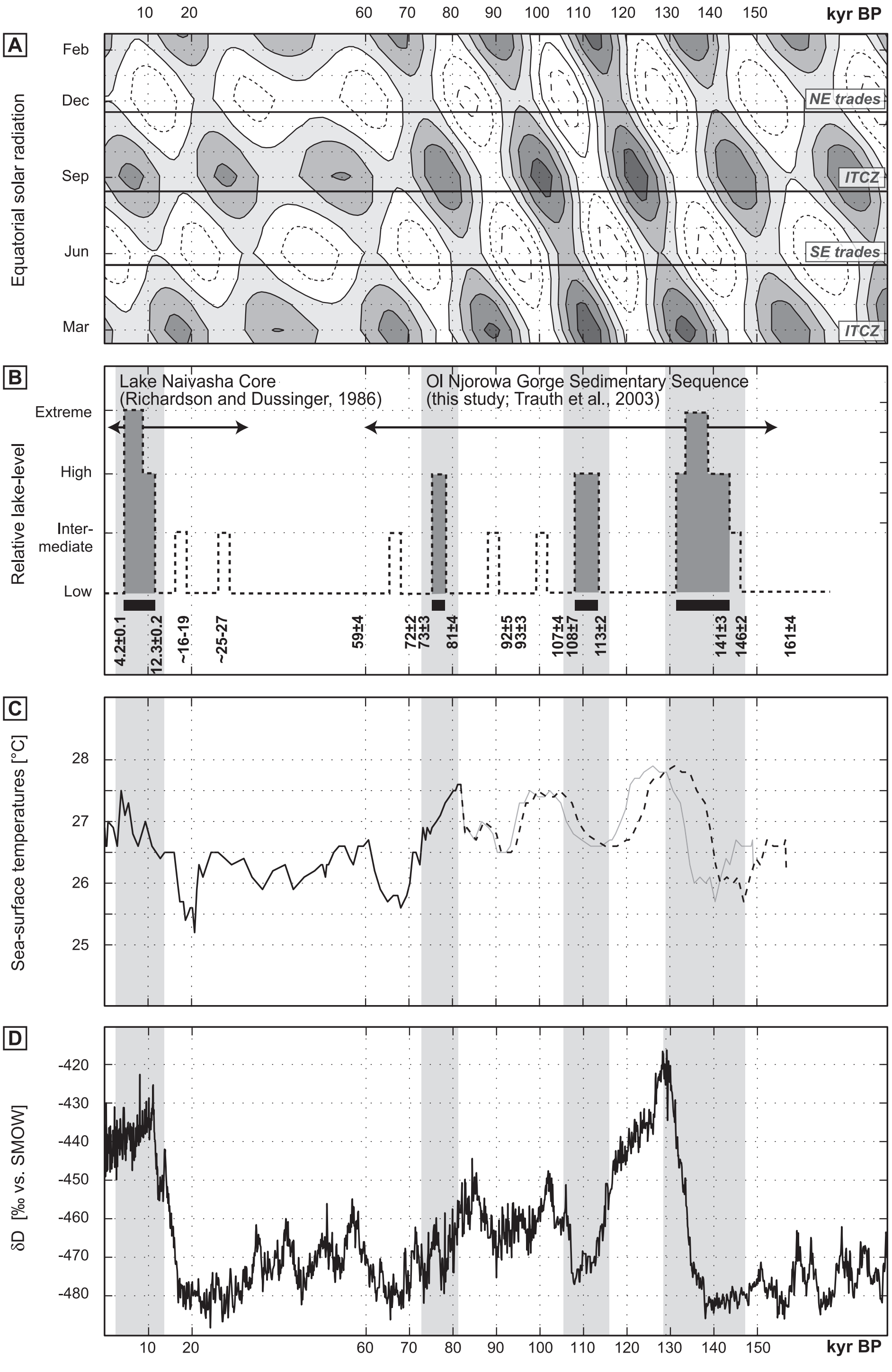
10
20
60
70
80
90
100
110
120
130
140
150
kyr BP
A
Equatorial solar radiation
Feb
Dec
Sep
Jun
Mar
NE trades
ITCZ
SE trades
ITCZ
B
Relative lake-level
Extreme
High
Inter-mediate
Low
Lake Naivasha Core
(Richardson and Dussinger, 1986)
Ol Njorowa Gorge Sedimentary Sequence
(this study; Trauth et al., 2003)
4.2±0.1
12.3±0.2
~16-19
~25-27
59±4
72±2
73±3
81±4
92±5
93±3
107±4
108±7
113±2
141±3
146±2
161±4
C
Sea-surface temperatures [°C]
28
27
26
25
D
δD [‰ vs. SMOW]
-420
-430
-440
-450
-460
-470
-480
10
20
60
70
80
90
100
110
120
130
140
150
kyr BP

balance in the catchment. The compilation suggests that the hydrological variations can best be explained by orbitally induced changes in solar radiation on the equator, but the lake-level fluctuations also correlate with variations in the Indian Ocean sea-surface temperatures (SSTs). Because the short-term variability of the present-day climate in East Africa is mainly controlled by such large-scale influences, changes of those factors provide a partial explanation of the hydrological fluctuations in the Central Kenya Rift.

Obviously, the chronology of lake-level highstands in the Naivasha basin at 10- to 11-kyr intervals follows the maximum in equatorial March and September insolation (cf. Trauth et al., 2003). The increased heating of the continent attracts more moisture to East Africa. In that context, both more intense spring and fall rainy seasons provoke higher water tables in the catchment. Interestingly, there is no one-to-one correlation between the amplitudes of maximum March and September insolation and the magnitude of the highstands. Moreover, assuming the chronology of our record is correct, significant differences between the timing of these highstands and solar-radiation maxima can be observed. We therefore believe that equatorial insolation is the most important but not the sole cause for hydrological changes in the Central Kenya Rift. Comparing our chronology with other Late Pleistocene-Holocene lake records in East Africa (Butzer et al., 1969; Hillaire-Marcel et al., 1986; Sturchio et al., 1993; Barker and Gasse, 2003) and tropical Indian-Ocean SST records as inferred from alkenones (Bard et al., 1997), periods of higher SSTs tend to correlate with the highest lake levels in East Africa. Higher ocean temperatures cause higher moisture availability and hence higher lateral water transport to the African continent. At present, lateral moisture transport during the short rains in fall is even stronger during ENSO-warm (i.e., El Niño) events (Camberlin, 1995; Nicholson, 1996, 2000; Indeje et al., 2000). In the past, periods of stronger ENSO as triggered by maximum lower latitude insolation may provide an additional source of increased humidity in the Central Kenya Rift (Clement et al., 1999; Beaufort et al., 2001; Stott et al., 2002). The rhythmic lamination of the diatomites provides some evidence for such an ENSO-type influence. This evaluation of the relative importance of changes of equatorial insolation, Indian and Pacific Ocean SSTs and their anomalies therefore confirms earlier work in the region and has important consequences for future models for climate–hydrology linkages in equatorial East Africa.

Acknowledgements

This project was funded by two grants to M. Trauth and M. Strecker by the German Research Foundation (DFG). We are grateful to the government of Kenya and the Kenya Wildlife Service for research permits and support. We furthermore acknowledge F. Gasse and F. Chalié for help with diatom taxonomy and interpretation as well as for friendly hospitality at CEREGE, the use of resources and many inspiring discussions. We thank the reviewers P. Barker, J. Halfman and T.C Johnson as well as our colleagues D. Verschuren and C. Brüchmann for discussions and helpful comments on the manuscript. We acknowledge S. Higgins, S. Kabingu and T. Schlüter for logistical support, C. Fischer for preparing thin sections, as well as G. Schlolaut and A. Renter for help with diatom preparation.

References

Bard, E., Rostek, F., Sonzogni, C., 1997. Interhemispheric synchrony of the last deglaciation inferred from alkenone paleothermometry. Nature 385, 707–710.

Barker, P., Gasse, F., 2003. New evidence for a reduced water balance in East Africa during the Last Glacial Maximum: implication for model-data comparison. Quaternary Science Reviews 22, 823–837.

Barker, P.F., Gasse, F., Roberts, N., Taieb, M., 1990. Taphonomy and diagenesis in diatom assemblages; a Late Pleistocene palaeoecological study from Lake Magadi, Kenya. Hydrobiologia 214, 267–272.

Battarbee, R.W., 2000. Paleolimnological approaches to climate change, with special regard to the biological record. Quaternary Science Reviews 19, 107–124.

Battarbee, R.W., Jones, V.J., Flower, R.J., Cameron, N.G., Bennion, H., Carvalho, L., Juggins, S., 2001. Diatoms. In: Smol, J.P., Birks, H.J.B., Last, W.M. (Eds.), Tracking Environmental Change using Lake Sediments, Terrestrial, Algal and Siliceous Ondicators vol. 3. Kluwer Academic Publishers, Dortrecht, pp. 155–202.

Beaufort, L., deGaridel-Thoron, T., Mix, A.C., Pisias, N., 2001. ENSO-like forcing on oceanic primary production during the Late Pleistocene. Science 293, 2440–2444.

Berger, A., Loutre, M.F., 1991. Insolation values for the climate of the last 10 million years. Quaternary Science Reviews 10 (04), 297–317.

Bergner, A.G.N., Trauth, M., Bookhagen, B., 2003. Paleoprecipitation estimates for the Lake Naivasha basin (Kenya) during the last 175 k.y. using a lake-balance model. Global and Planetary Change 36, 117–136.

Bradley, R.S., 1999. Paleoclimatology–reconstructing climates of the Quaternary. Academic Press. 511 pp.

Butzer, K.W., Brown, F.W., Thruber, D.L., 1969. Horizontal sediments of the lower Omo Valley; the Kibish formation. Quaternaria 11, 15–29.

Camberlin, P., 1995. June–September rainfall in North-Eastern Africa and atmospheric signals over the tropics: a zonal perspective. International Journal of Climatology 15, 773–783.

Chalié, F., Gasse, F., 2002. Late Glacial–Holocene diatom record of water chemistry and lake level change from the tropical East African Rift Lake Abiyata (Ethiopia). Palaeogeography, Palaeoclimatology, Palaeoecology 187, 259–283.

Clarke, M.C.G., Woodhall, D.G., Allen, D., Darling, G., 1990. Geological, volcanological and hydrogeological controls on the occurrence of geothermal activity in the area surrounding Lake Naivasha, Kenya. British Geological Survey Report and Govt. of Kenya — Ministry of Energy, Nairobi, Kenya.

Clement, A.C., Seager, R., Cane, M.A., 1999. Orbital controls on the El Niño/Southern Oscillation and the tropical climate. Paleoceanography 14, 441–456.

Damnati, B., Taieb, M., 1995. Solar and ENSO signatures in laminated deposits from Lake Magadi (Kenya) during the Pleistocene/Holocene transition. Journal of African Earth Sciences 21, 373–382.

Dühnforth, M., 2001. Rekonstruktion, Modellierung und Charakterisierung eines früh-holozänen Seespiegelhochstandes im Nakuru-Elmenteita-Becken Kenia. Unpublished diploma thesis, Humboldt-Universität Berlin.

Dühnforth, M., Bergner, A.G.N., Trauth, M.H., 2001. Hydrological modeling of the 10 kyr BP paleo-lake in the Nakuru-Elmenteita basin, Central Kenya Rift. Conference contribution to PAGES—PEP III meeting, August 27–31, Aix-en-Provence, .

Gasse, F., 1986. East African diatoms—taxonomy, ecological distribution. Bibliotheca Diatomologica vol. 11. Cramer, Stuttgart.

Gasse, F., 2000. Hydrological changes in the African tropics since the Last Glacial Maximum. Quaternary Science Reviews 19, 189–211.

Gasse, F., Van Campo, E., 2001. Late quaternary environmental changes from a pollen and diatom record in the southern tropics (Lake Tritvakely, Madagascar). Palaeogeography, Palaeoclimatology, Palaeoecology 167, 287–308.

Gasse, F., Juggins, S., Ben Khelifa, L., 1995. Diatom-based transfer functions for inferring past hydrochemical characteristics of African lakes. Palaeogeography, Palaeoclimatology, Palaeoecology 117, 31–54.

Gasse, F., Barker, P., Gell, P.A., Fritz, S.C., Chalié, F., 1997. Diatom-inferred salinity in paleolakes: an indirect tracer of climate change. Quaternary Science Reviews 16, 547–563.

Gaudet, J.J., Melack, J.M., 1981. Major ion chemistry in a tropical lake basin. Freshwater Biology 11, 309–333.

Hecky, R.E., Kilham, P., 1973. Diatoms in alkaline, saline lakes: ecology and geochemical implications. Limnology and Oceanography 18 (1), 53–71.

Hillaire-Marcel, C., Carro, O., Casanova, J., 1986. 14C and Th/U dating of Pleistocene and Holocene stromatolites from East African paleolakes. Quaternary Research 25, 312–329.

Hustedt, F., 1949. Süßwasserdiatomeen aus dem Albert-Nationalpark in Belgisch Kongo. In: Damas, H. (Ed.), Exploration du Parc National Albert (1935–1936). Hayez, Bruxelles. 199 pp.

Indeje, M., Semazzi, F.H.M., Ogallo, L.J., 2000. ENSO signals in East African rainfall seasons. International Journal of Climatology 20, 19–46.

Jätzold, R., 1981. Klimageographie—Ostafrika, Kenya, Uganda, Tanzania 2°N–2°S, 32°–38°E. In: Freitag, U. (Ed.), Afrika-Kartenwerk, Serie E, Beiheft zu Blatt 5. Bornträger, Berlin. 117 pp.

Kenya Meteorological Department, 2000. Unpublished synoptic and rain station data. Ministry of Information, Transport and Communications, Nairobi, Kenya.

Krammer, K., Lange-Bertalot, H., 1991a. Bacillariophyceae—3. Teil: Centrales, Fragilariaceae, Eunotiaceae. In: Ettl, H., Gerloff, J., Heynig, H., Mollenhauer, D. (Eds.), Süßwasserflora ßwasserflora von Mitteleuropa vol. 2/3. Gustav Fischer, Stuttgart. 596 pp.

Krammer, K., Lange-Bertalot, H., 1991b. Bacillariophyceae—4. Teil: Achnanthaceae, kritische ergänzungen zu navicula (lineolatae) und gomphonema, gesamtliteraturverzeichnis teil 1–4. In: Ettl, H., Gerloff, J., Heynig, H., Mollenhauer, D. (Eds.), Süßwasserflora von Mitteleuropa vol. 2/4. Gustav Fischer, Stuttgart. 437 pp.

Krammer, K., Lange-Bertalot, H., 1997a. Bacillariophyceae—1. Teil: Naviculaceae. In: Ettl, H., Gerloff, J., Heynig, H., Mollenhauer, D. (Eds.), Süßwasserflora von Mitteleuropa vol. 2/1. Gustav Fischer, Stuttgart. 876 pp.

Krammer, K., Lange-Bertalot, H., 1997b. Bacillariophyceae—2. Teil: Bacillariaceae, Epithemiaceae, Surirellaceae. In: Ettl, H., Gerloff, J., Heynig, H., Mollenhauer, D. (Eds.), Süßwasserflora von Mitteleuropa vol. 2/2. Gustav Fischer, Stuttgart. 576 pp.

Nicholson, S.E., 1996. A review of climate dynamics and climate variability in Eastern Africa. In: Johnson, T.C., Odada, E. (Eds.), The Limnology, Climatology and Paleoclimatology of the East African Lakes, The International Decade for the East African Lakes (IDEAL). Gordon and Breach Publishers, pp. 25–56.

Nicholson, S.E., 2000. The nature of rainfall variability over Africa on time scales of decades to millenia. Global and Planetary Change 26, 137–158.

Nilsson, E., 1931. Quaternary glaciations and pluvial lakes in British East Africa. Geographiska Annaler 13, 249–349.

Ojiambo, B.S., Lyons, W.B., 1996. Residence time of major ions in Lake Naivasha, Kenya, and their relationship to Lake Hydrology. In: Johnson, T.C., Odada, E. (Eds.), The Limnology, Climatology and Paleoclimatology of the East African Lakes, The International Decade for the East African Lakes (IDEAL), pp. 267–278.

Owen, R.B., 2002. Sedimentological characteristics and origins of diatomaceous deposits in the East African Rift system. SEPM Special Publication 73, 233–246.

Petit, J.R., Jouzel, J., Raynaud, D., Brkov, N.I., Barnola, J.-M., Basile, I., Bender, M., Chappellaz, J., Davis, M., Delaygue, G., Delmotte, M., Kotlyakov, V.M., Legrand, M., Lipenkov, V.Y., Lorius, C., Pépin, L., Ritz, C., Saltzmann, E., Stievenard, M., 1999. Climate and atmospheric history of the past 420,000 years from the Vostok ice core, Antarctica. Nature 399, 429–436.

Richardson, J.L., Dussinger, R.A., 1986. Paleolimnology of mid-elevation lakes in the Kenya Rift Valley. Hydrobiologia 143, 167–174.

Richardson, J.L., Richardson, A.E., 1972. History of an African rift lake and its climatic implications. Ecological Monographs 42 (4), 499–534.

Roberts, N., Taieb, M., Barker, P., Damnati, B., Icole, M., Williamson, D., 1993. Timing of the Younger Dryas event in East Africa from lake-level changes. Nature 366, 146–148.

Robbins, J.A., Krezoski, J.R., Mozley, S.C., 1977. Radioactivity in sediments of the great lakes: post-depositional redistribution by deposit-feeding organisms. Earth and Planetary Science Letters 36, 325–333.

Saji, N.H., Goswami, B.N., Vinayachandran, P.N., Yamagata, T., 1999. A dipole mode in the tropical Indian Ocean. Nature 401, 360–363.

Shackleton, N.J., Sanchez-Goñi, M.F., Pailler, D., Lancelot, Y., 2003. Marine isotope substage 5e and the eemian interglacial. Global and Planetary Change 36, 151–155.

Smol, J.P., Birks, H.J.B., Last, W.M. (Eds.), Tracking Environmental Change using Lake Sediments, Terrestrial, Algal and Siliceous Ondicators vol. 3. Kluwer Academic Publishers, Dortrecht.

Stager, J.C., Johnson, T.C., 2000. A 12,400 ^{14}C yr offshore diatom record from east central Lake Victoria, East Africa. Journal of Paleolimnology 23, 373–383.

Stott, L., Poulsen, C., Lund, S., Thunell, R., 2002. Super ENSO and global climate oscillations at millennial time scales. Science 297, 222–226.

Sturchio, N.C., Dunkley, P.N., Smith, M., 1993. Climate-driven variations in geothermal activity in the northern Kenya rift valley. Nature 362, 233–234.

Swan, A.R.H., Sandilands, M., 1995. Introduction to Geological Data Analysis. Blackwell Sciences, Oxford. 446 pp.

Tarras-Wahlberg, H., Everard, M., Harper, D.M., 2002. Geochemical and physical characteristics of river and lake sediments at Naivasha, Kenya. Hydrobiologia 488 (1–3), 27–41.

Taub, F.B., 1996. Lakes reservoirs. Ecosystems of the world, vol. 23. Elsevier, Amsterdam. 643 pp.

Telford, R.J., Lamb, H.F., 1999. Groundwater-mediated response to holocene climatic change recorded by the diatom stratigraphy of an Ethiopian crater lake. Quaternary Research 52, 63–75.

Trauth, M.H., Strecker, M.R., 1996. Late Pleistocene Lake-Level Fluctuations in the Naivasha Basin, Kenya. In: Johnson, T.C., Odada, E. (Eds.), The Limnology, Climatology and Paleoclimatology of the East African Lakes, The International decade for the East African Lakes (IDEAL), pp. 549–557.

Trauth, M.H., Deino, A., Strecker, M.R., 2001. Response of the East African climate to orbital forcing during the Last Interglacial (130–117 kyr BP) and the early Last Glacial (117–60 kyr BP). Geology 29 (6), 499–502.

Trauth, M.H., Deino, A.L., Bergner, A.G.N., Strecker, M.R., 2003. East African climate change and orbital forcing during the last 175 kyr BP. Earth and Planetary Science Letters 206, 297–313.

Verschuren, D., 1999. Sedimentation controls on the preservation and time resolution of climate-proxy records from shallow fluctuating lakes. Quaternary Science Reviews 18, 821–837.

Washbourn-Kamau, C.K., 1975. Late Quaternary shorelines of Lake Naivasha, Kenya. Azania X, 77–92.

Washbourn-Kamau, C.K., 1977. The Ol Njorowa Gorge, Lake Naivasha basin, Kenya. In: Greer, D.C. (Ed.), Desertic Terminal Lakes. Utah Water Research Laboratory, pp. 297–307.

Wetzel, R.G. (Ed.), Limnology. Academic Press, London. 841 pp.

Wise, B.M., Gallagher, N.B., Bro, R., Shaver, J.M., 2002. PLS Toolbox for Use with Matlab, version 3.0, software. Eigenvector Research.